Research & Reviews: Journal of Chemistry

e-ISSN:2319-9849
p-ISSN:2322-0082

Electrochemical Sensors Using Nanomaterials - A Mini Review

Tanimu A*, Lawal MA and Getso ZN

Ahmadu Bello University, Zaria, Nigeria

Review Article

Received date: 09/09/2017
Accepted date: 18/10/2017
Published date: 29/10/2017

***For Correspondence**

Abdulkadir Tanimu, Ahmadu Bello University, Zaria, Nigeria.
Tel: +2348032925161

E-mail: abdulkadir_tanimu@yahoo.com

Keywords: Nanotechnology; Electrohemical sensors; Catalysis

ABSTRACT

Nanotechnology has been in recent years an indispensable tool for great advancement in science and technology. With advanced preparatory methods, nanomaterials can have the desired size control, surface properties, shape and other physicochemical properties. Their larger surface area to volume ratio, which offers them the capacity to improve electron-transfer rate are quite utilized in catalysis, polymer technology, drug delivery, food production, painting and electrochemical sensing. Since electrochemical sensors are required to be of very high sensitivity, selectivity and stability, incorporation of nanomaterials in the sensors' design is inevitable due to their aforementioned properties. So many work have therefore been reported in which nanomaterials ranging from nanoparticles to nanotubes were used for improving the properties of sensors and the results of these researches have been so far promising. This article therefore intends to present some of these works and showcase the relevance of nanomaterials in electrochemical sensor developments.

INTRODUCTION

Nanomaterials and nanotechnology have grown over the years and still stands as an indispensable technology for great advancement in science and technology. Nanomaterials are basically materials that have one of their dimensions less than or equal 100 nanometer scale [1-4]. Advancement in the synthesis methodologies of these nanomaterials now permits preparation of variety of the materials with the desired size, surface properties, shape and other physicochemical properties [5-7]. Moreover, the materials can be functionalized thus offering great prospect for combining biological recognition events and signal transduction mechanism in developing novel bioelectronic devices with excellent sensor properties [8-13]. Nanomaterials generally have larger surface area, the ability to improve the electron-transfer rate and these properties among others are quite utilized in catalysis [14], polymer technology [15], drug delivery [16], food production [17], painting [4] and electrochemical sensing [18]. Electrochemical sensors forms an integral subdivision of chemical sensors in which the transduction element is designed from an electrode [19,20]. It basically work on the principle of electrochemistry, which is also a very powerful electroanalytical technique that has the advantages of high sensitivity, instrument simplicity, portability, easy miniaturization and relatively low cost [21]. Recently, portable biochemical detection was made possible through the use of smartphones integrated with sensors, such as test trips, sensor chips and hand-held detectors [22]. The integration of these miniaturized devices as sensitive arrays was possible through the application of micro-electro-mechanical systems and of course nanotechnology [23-25]. Since some of the properties of sensors are very high sensitivity, selectivity and stability, researchers have in recent years put a lot of effort towards improving these properties and one of the ways is the incorporation of nanomaterials in the sensors. The aim of this review is to expose researchers to the success recorded in this area while hoping that the article will stimulate further discoveries in the area of electrochemical sensors using nanomaterials.

QUANTUM-DOT NANOMATERIAL

These are nanocrystals with excellent electrical and optical properties [26,27]. Quantum-dot (QD) semiconductor nanocrystals have been reported to be used for design of multi-analyte electrochemical aptamers biosensor with subpico molar (attomole) detection limit [28]. Aptamer is the RNA or DNA ligand to the target molecule and it was usually obtained by the method called 'systematic evolution of ligands by exponential enrichment (SELEX) [29]. The aptamers can bind strongly to a target molecule like an antibody and can be tailored with high degree of efficiency and as such are used as powerful tool for proteome analysis [30]. Other advantages are its relative ease of isolation and modifications coupled with high stability. The nanocrystals play

e-ISSN:2319-9849
p-ISSN:2322-0082

the significant role of electro diversification of the electrical tags, one of the requirements for multiplexed bioanalysis and the remarkable low (attomole) detection limit therefore is a consequence of the extensive amplification quality of the nanoparticle-based electrochemical stripping measurements [31]. Since it is multi-analyte biosensor, four different encoding nanomaterials, CdS; ZnS; CuS; and PbS, were used to differentiate the signals of four targeted DNA. In operating the aptamer/Quantum-Dot-Based dual-analyte biosensor, single-step displacement assay was used as presented in **Scheme 1**.

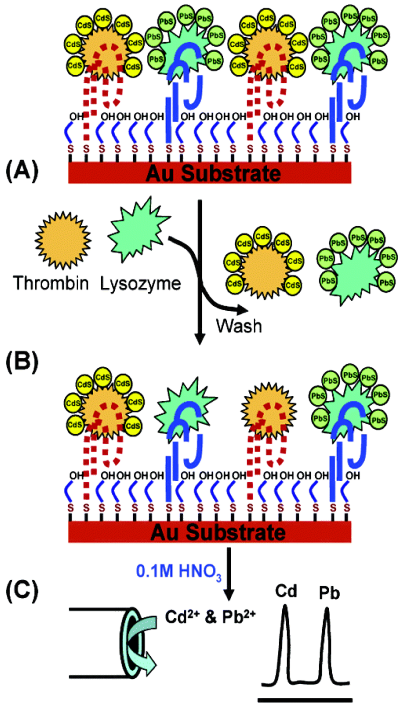

Scheme 1. Operation of the Aptamer/Quantum-Dot-based dual-analyte biosensor involving displacement of the tagged proteins by the target analytes, (A) Mixed monolayer of thiolated aptamers on the gold substrate with the bound protein–QD conjugates; (B) sample addition and displacement of the tagged proteins; (C) dissolution of the remaining captured nanocrystals followed by their electrochemical-stripping detection at a coated glassy carbon electrode. Adapted from [28].

In the scheme, several thiolated aptamers were co-immobilized, together with binding of the matching QD-tagged proteins on the gold substrate (A), followed by sample addition (B) and displacement of the tag proteins. The displacement, allows monitoring of the remaining nanocrystals via electrochemical detection means (C). The biosensor was first used for single analyte sensing in order to assess its sensitivity and selectivity. High sensitivity accrued from the electrochemical detection was shown in **Figure 1a** and the calibration plot, presented in **Figure 1b** depicts a rapid drop in the peak current up to 200 ng L^{-1} which later maintained a slower decrease, typical of displacement assays. Detection limit of 20 ng L^{-1} (0.5 pM) was recorded within the concentration range of 20 to 500 ng L^{-1}. The biosensor therefore, has much lower detection limit (of the order of 3-4) than those aptamer biosensors reported previously [32-34]. High reproducibility (relative standard deviation of 5%) was recorded after six consecutive measurements of 100 ngL^{-1} thrombin.

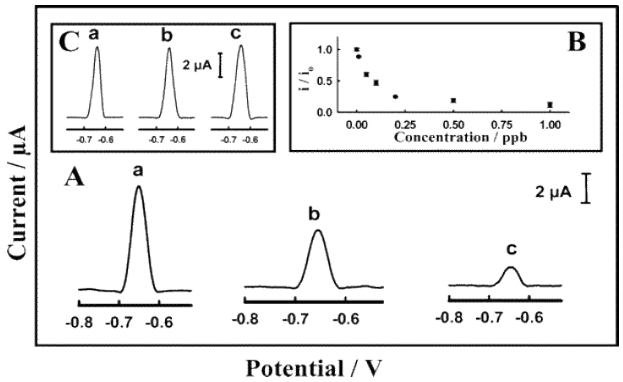

Figure 1. (A) Square-wave stripping voltammograms for different concentrations of thrombin: 0 (a), 100 (b), and 500 (c) ng L^{-1}. (B) The resulting calibration plot. (C) Assessment of the selectivity using nontarget proteins: (a) control (no analyte or interference), (b) 25 μg L^{-1} BSA, and (c) 25 μg L^{-1} IgG. Dissolution of the QDs (conjugated to the undisplaced protein molecules) was carried out by the addition of HNO_3 (100 μL, 0.1 M) and sonication for 1 h. The resulting solution was transferred to a 1 mL electrochemical cell containing 900 μL of acetate buffer (0.1 M, pH 4.6) and 10 ppm mercury (II). Electrochemical stripping detection proceeded after 1 min pretreatment at +0.6 V, 2 min accumulation at -1.2 V, and scanning the potential to -0.25 V. Adapted from [28].

e-ISSN:2319-9849
p-ISSN:2322-0082

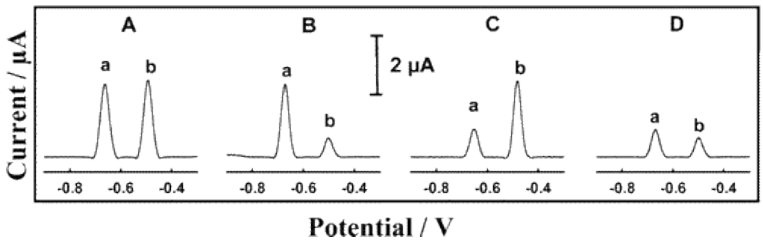

Figure 2. Simultaneous bioelectronic detection of lysozyme and thrombin. Square-wave stripping voltammograms obtained after additions of (A) 0 µg L^{-1} protein, (B) 1 µg L^{-1} lysozyme, (C) 0.5 µg L^{-1} thrombin, and (D) a mixture of 1 µg L^{-1} lysozyme (a) and 0.5 µg L^{-1} thrombin (b). Conditions as in **Figure 1**. Adapted from [28].

The multi-analyte task of the biosensor was demonstrated in **Figure 2**, where dual-analyte detection of thrombin (a) and lysozyme (b) were presented. Similar reductions in both metal peaks was a consequence of the simultaneous addition of both thrombin and lysozyme proteins as in **Figure 2d**. This suggest that if there are non-overlapping metal peaks within a given potential window, then as much as five or six protein targets can be analyzed simultaneously in a single run. CdS nanoparticle-based (another Quantum-Dot) bio sensing of sugars based on their interaction with surface-functionalized lectins was also presented in **Scheme 2** [35]. This is achieved by immobilization of lectin, the recognition element for carbohydrate, onto the gold surface and contention between a nanocrystal (CdS)-labeled sugar and target sugar for carbohydrate binding sites on lectins was monitored through highly sensitive electrochemical stripping detection of the captured nanocrystal.

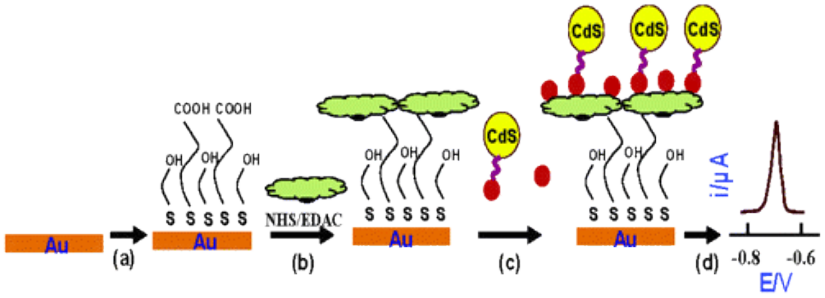

Scheme 2. Operation of the Nanoparticle-Based Bioelectronic Sensor for Glycans Involving Competition of the Tagged Sugar with the Target Analytes for the Binding Sites of the Immobilized Lectin, (a) Mixed self-assembled monolayer on the gold substrate; (b) covalent immobilization of the lectin; (c) addition of the tagged and untagged sugars; (d) dissolution of the captured nanocrystals, followed by their stripping-voltammetry detection at a mercury-coated glassy carbon electrode. Adapted from [35].

The lectin-sugar recognition event thus yields a distinct cadmium stripping voltammetry current peak, whose size depends inversely on the level and affinity of the target glycan. A model system involving a surface-bound pure *Arachis hypogaea* (peanut agglutinin, PNA) lectin and various analytes was used to optimize and test the assay, and excellent selectivity for targeted analytes was observed as presented in **Figure 3**. The sensitivity trend, β-D-Gal-[1→3] [36]-D-GalNAc>Gal>GalNAc, was found consistent with the reported relative affinity of these carbohydrate moieties to PNA lectin [37]. Interestingly, even with excess amount of non-target sugars such as glucose and mannose, no response was observed **(Figures 3e and 3f)**. This makes Lectin array a successful distinguisher of individual sugars [35]. Square-wave voltammetric signals for different concentrations of the target β-D-Gal-[1→3]-D-GalNAc glycan was presented in **Figure 4d** and distinctly smaller cadmium stripping peaks, corresponding to smaller levels of the captured CdS-tagged sugar, was observed with increasing concentration of the target.

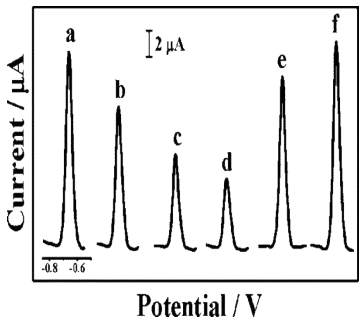

Figure 3. Square-wave voltammetry stripping signals in the presence of (a) "control" solution (no target), (b) 11.1 µM GalNAc, (c) 11.1 µM Gal, (d) 11.1 µM β-d-Gal-[1→3]-d-GalNAc, (e) 277 µM glucose, and (f) 277 µM mannose. Incubation time, 60 min. Dissolution of the QDs (conjugated to the lectin-bound sugar molecules) was carried out by adding 100 µL nitric acid (0.1 M) and incubating for 60 min. The resulting solution was transferred to the electrochemical cell containing 300 µL of acetate buffer (0.1 M, pH 5.3) and 10 ppm Hg^{2+}. Electrochemical stripping detection proceeded using an 8 min deposition at -1.1 V and scanning the potential to -0.2 V using an amplitude of 25 mV, a potential step of 4 and a frequency of 25 Hz. Concentration of the tagged sugar [CdS-(4-aminophenol-β-d-galactopyranoside)], 800 µg L^{-1}. Adapted from [35].

e-ISSN:2319-9849
p-ISSN:2322-0082

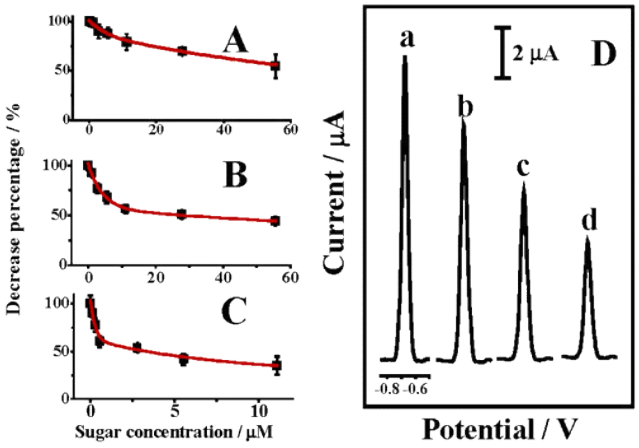

Figure 4. Corresponding calibration plots of (A) GalNAc, (B) Gal, and (C) β-d-Gal-[1⟶3]-d-GalNAc. (D) Square-wave voltammetry stripping signals in the presence of (a) 0.0, (b) 0.277, (c) 2.77, and (d) 11.1 μM β-d-Gal-[1⟶3]-d-GalNAc. Other conditions, as in **Figure 3**. Adapted from [35].

The detection limit for β-D-Gal-[1⟶3]-D-GalNAc, determined from the calibration plot in **Figure 4c**, was 0.1 μM, corresponding to 38.3 ng mL^{-1}. Also presented were the calibration plots of GalNAc **(Figure 4a)** and Gal **(Figure 4b)**, with 2.7 μM and 1 μM detection limits respectively. The trend in sensitivity was found consistent with square-wave voltammetric stripping analysis in **Figure 3**. Reproducibility test for the bioassay was found to be good from the 5.7% relative standard deviation result for six series of repetitive measurements of 27.7 μM GalNAc. The article also reported optimization of CdS-tagged sugar over a concentration range of 0.2-1.5 μg mL^{-1} and optimum response was achieved at 0.8 μg mL^{-1} concentration. Incubation time was also optimized by varying the time over a range of 20-120 min in the presence and absence of target sugar and in both cases optimum incubation time of 80 min was achieved.

GOLD NANOPARTICLES

Gold nanoparticles (AuNPs) attracted many attentions in electrochemical sensors due to their large surface area to volume ratio, good electrical properties, high surface reaction activity, small particle size and good surface properties [7,38-40]. In an attempt to have an amplified electrical transduction of DNA, Kawde and Jang had developed a polymeric beads consisting of large number of nanoparticles [41]. **Scheme 3** presented the analytical protocol, which involved the hybridization of oligonucleotide probe (captured on magnetic beads) to the DNA target labeled with the gold-loaded carrier sphere (a), followed by subsequent dissolution (c) and detection via stripping potentiometry (d) of the gold tracer disposable thick-film carbon electrode.

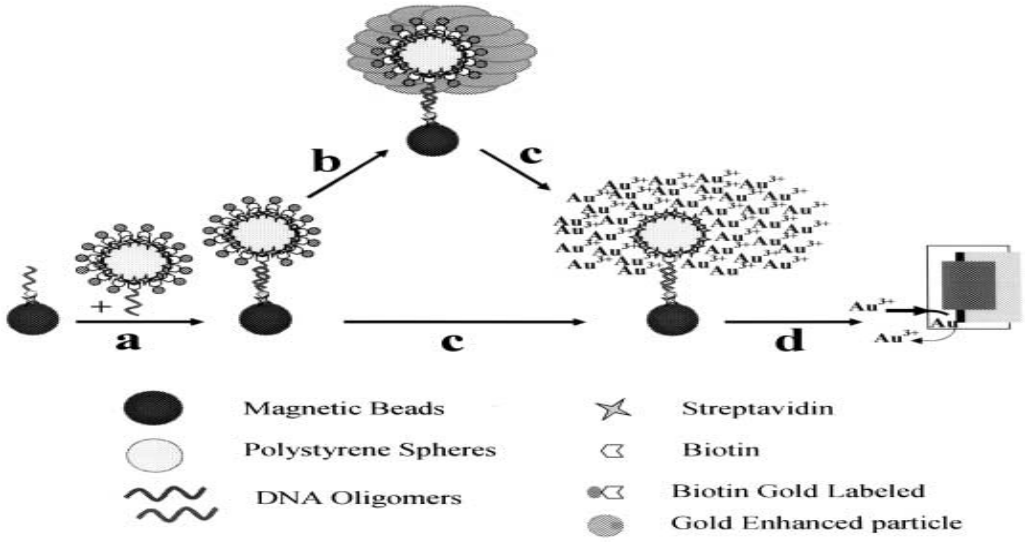

Scheme 3. Amplified analytical protocol. a) hybridization event; b) catalytic enlargement; c) gold dissolution; d) stripping detection. Adapted from [41].

Thus, higher amplification, courtesy of the combined use of carrier-bead and highly sensitive electrochemical stripping detection of the multiple AuNPs tracers was obtained. Much higher sensitivity was achieved by incorporating catalytic enlargement of the multiple gold-particle tags in addition to the carrier bead amplifying units and the ultrasensitive electrochemical stripping detection **(Scheme 3b)**. Structural and morphological insight of the gold-loaded polymeric beads indicated duplex formation

e-ISSN:2319-9849
p-ISSN:2322-0082

results in linking of the approximately 0.6 µm polystyrene spheres to the approximately 0.8 µm magnetic beads. TEM micrograph allows clear sight of each and every gold nanoparticle on the polystyrene carrier beads before and after enhancement. The gold loading time was optimized to 15 min loading time for 1 × 10^{11} gold particles solution. Chrono potentiometric stripping hybridization response of the new protocol exhibit unimaginably larger gold signal for lower target concentration **(Figures 5a and 5b)**, as compared with the traditional assay [42]. However, no response was observed for a 1000-fold excess of non-complementary DNA **(Figure 5c)**. Concentration effect in the ultralow DNA concentration range of 100-500 ng mL^{-1} showed a nonlinear peak area increment with the increasing target concentration. However, the logarithmic plot in **Figure 6** was found linear over the entire concentration range used. Similar behavior was reported in other particle-based bioassays [42,43] and agrees with models of particle aggregation involving avidin/biotin systems [44]. From the calibration plot, the limit of detection was calculated to be 40 pg mL^{-1} (6 pM) on the S/N=3 for the response of 100 pg mL^{-1} target DNA, which is much lower than the conventional single-particle stripping hybridization assay detection limit of 100 ng mL^{-1} [42,45,46]. Good reproducibility was achieved after six consecutive repetitive measurements of the 100 ng mL^{-1} targeted DNA. Graphene quantum dots (GQD) functionalized gold nanoparticles (AuNPs) were reported to show extraordinary performance in the ultralow detection of Hg^{2+} and Cu^{2+} coupled with high sensitivity [47]. This was achieved by drop-casting of the GQD-AuNPs onto a polished glassy carbon electrode and using anodic stripping voltammetry, the square wave voltammogram was recorded. 3D-AuNPs-Graphene composite was also applied in electrochemical immunoassay for carcinoembryonic antigen through utilization of the large surface area of gold nanoparticles which enabled capturing of more primary antibodies at the same time improving the electronic transmission rate [48].

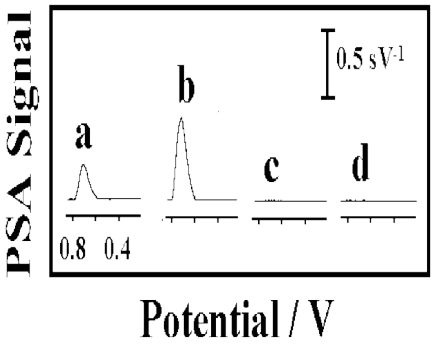

Figure 5. Chronoamperometric stripping hybridization response of the single- (a) and multi- (b-d) particle protocols to 500 ng mL^{-1} target(a), 1 ng mL^{-1} target (b), to 1000 ng mL^{-1} non-complementary DNA (c), and control solution containing 20 µg gold-tagged beads (d). Adapted from [41].

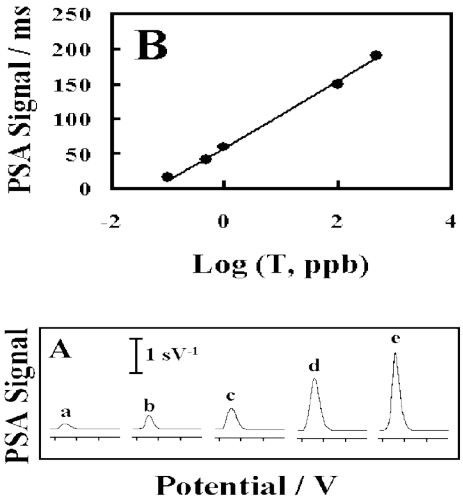

Figure 6. Chronoamperometric signal for increasing level of E908X-WT DNA: 0.1(a), 0.5(b), 1.0(c), 100(d) and 500 (e) ng mL^{-1}. Adapted from [41].

MULTI-WALLED NANOTUBES

Multi-walled nanotubes (MWNTs) is a subclass of carbon nanotubes, which are new types of carbon materials formed from the folding of graphene layers into carbon cylinders [49,50]. Their special geometry, unique electronic, mechanical, chemical and thermal properties made them highly attractive for electrochemical applications [51]. Wang et al. had developed a novel biosensor for glucose detection based MWNTs [52]. The MWNT-based enzyme electrode was designed by growing the MWNTs on Si substrate, then followed by evaporating on the top surface of the MWNTs a thin gold film. Later the substrate was completely removed by etching with mixture of HNO_3 and HF. This provide amble surface for the glucose oxidase to attach to, hence providing the extra sensitivity. The glucose oxidase enzymes mediate the direct electron transfer to the gold transducer and produce the response current. Detail of the chemical reaction is shown below [53]:

e-ISSN:2319-9849
p-ISSN:2322-0082

$$Glucose+O_2 \rightarrow gluconic\ acid+H_2O_2 \quad (1)$$

$$and\ H_2O_2 \rightarrow 2H^+ + O_2 + 2e^- \quad (2)$$

Amperometry response of MWNT-based biosensor to glucose together with glassy carbon biosensor shows that MWNT-based biosensor exhibits much stronger response to glucose than glassy carbon biosensor. More interestingly, is at a fixed potential of +0.45 V vs Ag/AgCl, no response was observed with glassy carbon biosensor, whereas MWNT-based biosensor gave a good signal. This further buttress the higher sensitivity of the MWNT-based biosensor, a property acquired due to the nanomaterials that permit immobilization of more glucose oxidase enzymes [54]. In terms of stability of the biosensors, MWNT-based retained 86.7% of its initial activity after storing in a buffer solution at 4˚C for four months, however, 37.2% initial activity was retained for glassy carbon biosensor under the same conditions. Multi-walled carbon nanotubes hybrid in conjugation with other electrochemically active materials such as graphene oxide, metal nanoparticles etcetera, have been utilized in several electrochemical discoveries ranging from biological to environmental applications [55-58].

ZnO NANOTUBES

Recently, ZnONTs have numerous application in electrochemical biosensors due to its biocompatibility, non-toxicity, fast electron-transfer rate and easy application [59,60]. ZnO nanotubes (ZnONTs) has also been reported for application in glucose detection [18]. The work was designed based on the same principle of glucose oxidation by glucose oxidase enzyme. Experimental parameters such as voltage, pH and temperature were optimized before the amperometric detection of glucose and it was observed that, voltage=0.8 V, pH=7 and temperature=50˚C were the optimum conditions, however, temperature of 25˚C was used throughout the analysis in order to avoid evaporation of solvents. The ZnONT-based biosensor was reported to respond faster and sensitively to glucose in PB solution. Calibration plot for different glucose concentration response showed straight line and the linear response range was from 50 µM to 12 mM. The sensitivity and LOD were determined to be 21.7 µA/mMcm^2 and 1 µM (S/N=3) respectively. The authors tried to compare the sensitivity of ZnONT with ZnO nanorods (ZnONR) and Au film. In all cases, ZnONT stand out to be the best and this was attributed to the structure of ZnONT which provides higher electrode surface area for glucose oxidase immobilization. The effect of interference by some electroactive species such as ascorbic acid, L-Cysteine and urea were performed and little or no response was recorded for both L-Cysteine and urea while ascorbic acid showed current increment of 9.0% which is still insignificant considering its concentration in physiological condition [61], thus provide negligible effect for glucose determination in serum sample. Relative standard deviation of 2.2% was recorded for 13 continuous assays and a long-term stability of 70% of initial response after 60 days 90% of initial response after three weeks were recorded. ZnO also found application in ethanol gas sensing, for example, recently zinc oxide (ZnO) nanorods synthesized via low temperature hydrothermal process was utilized to construct ethanol gas sensor at different operating temperature by measuring the output voltage signal and has demonstrated high, reversible and fast response to ethanol [62]. In an attempt to improve the sensor performance, the ZnO was later grown 90˚ to the axis of tin oxide (SnO_2) nanowires synthesized by thermal evaporation, to form a hierarchical nanostructures [63] and it was revealed that hierarchical nanostructures enhanced the ethanol gas response and selectivity for interfering gases such as NH_3, CO, H_2, CO_2, and LPG. Platinum and palladium doped ZnO nanoarrays were also shown to be self-powered active ethanol gas sensors at room temperature by uniformly distributing the metal nanoparticles on the surface of the ZnO nanowire [64,65]. The room-temperature self-powered ethanol sensing behavior was attributed to the catalytic effect of the metal nanoparticles, the Schottky barrier at the metal/ZnO interface, and the piezotronics effect of the ZnO nanowires. Single crystalline Zinc sulfide nanowires grown by thermal evaporation have also shown high sensitivity, fast response and recovery times, and high selectivity towards detection of acetone and ethanol down to 500 ppb level [66].

NICKEL OXIDE NANOPARTICLES AND CARBON BLACK

A glassy carbon electrode modified with Nickel oxide nanoparticles (NiONPs) and carbon black was reported to be simple and highly selective electrode for combined determination of paracetamol (PCT) and codeine (COD) [67]. The NiONPs are important nanomaterials due to their specific chemical, surface and microstructural properties [68]. NiONPs were electrodeposited on a carbon black-dihexadecylphosphate (CB-DHP) dispersed glassy carbon electrode, forming the NiONPs-CB-DHP/GCE electrode as the indicator electrode. The NiONPs-CB-DHP/GCE was electrochemically characterized using cyclic voltammetry and optimization of the electrochemical behavior of target analytes were carried out using cyclic voltammetry and square wave voltammetry. The cyclic voltammograms for NiONPs-CB-DHP/GCE presented in **Figure 7** shows a reversible process after different scan rates, which confirmed the formation of NiONPs on the electrode surface. The reversible process is based on the equation below:

$$Ni(OH)_2 + OH^- \leftrightarrow NiO(OH) + H_2O + e^- \quad (3)$$

The electrochemical behavior of PCT and COD shows a synergic effect upon incorporation of NiONPs to the CB-DHP/GCE electrode for both PCT and COD due to the increase in the analytical signal. The increased signal was attributed to the chemical interaction between the NiONPs and the -OH groups present in the drug structures [69].

e-ISSN:2319-9849
p-ISSN:2322-0082

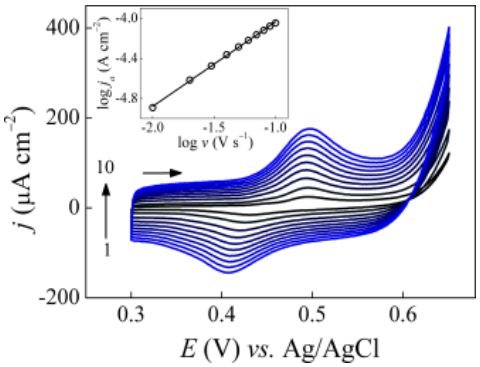

Figure 7. Cyclic voltammograms obtained for the NiONPs-CB-DHP/GCE in 0.1 mol L^{-1}NaOH solution at different scan rates:(1-10): 10, 20, 30, 40, 50, 60, 70, 80, 90 and 100 mV s^{-1}. Inset: log j_a *vs.* log *v*. Adapted from [67].

Effect of pH for the detection of the PCT and COD using the NiONPs-CB-DHP/GCE electrode was investigated by varying pH between the range of 2.0-7.0 and it was observed that for PCT increase in pH resulted to a negative shift in potential for the anodic and cathodic peak current. However, COD showed largest current signal at pH of 3, thus BR buffer solution at pH 3.0 was used for further analysis. Electrochemical behavior to various supporting electrolytes was also investigated using 0.04 molL^{-1} BR buffer (pH 3.0), 0.1 molL^{-1} phosphate buffer (pH 3.0) and 0.1 molL^{-1} KNO_3 solution (pH 3.0, adjusted with a 0.5 mol L^{-1} HNO_3 solution). Best analytical signals were obtained with BR buffer solution. The response of PCT and COD in the presence of each other was then carried out after the optimization using square wave voltammetry, in first case keeping a constant COD concentration and varying the concentration of PCT and in the second case, the vice versa. **Figures 8a and 8b** showed both variables have increase response with increase concentration while the response of the fixed analyte remain practically constant and it was confirmed that with both PCT and COD in the same solution, they do not interfere with each other. Then the authors carried out the simultaneous addition of the different concentrations of the analytes and the limit of detection for both analytes were determined to be 012 μmolL^{-1} for PCT and 0.48 μmolL^{-1} for COD (S/N=3) (see **Figure 9**). The intra-day repeatability after ten successive measurements and inter-day repeatability after three consecutive days gave RSD of 3.7% for PCT and 7.8% for COD and 8.8% for both PCT and COD respectively. Interferences effect due to sodium benzoate, silicon dioxide, EDTA, sodium bisulfide, magnesium stearate, starch and cellulose was evaluated and it was found that there was no significant interference in the simultaneous detection of PCT and COD.

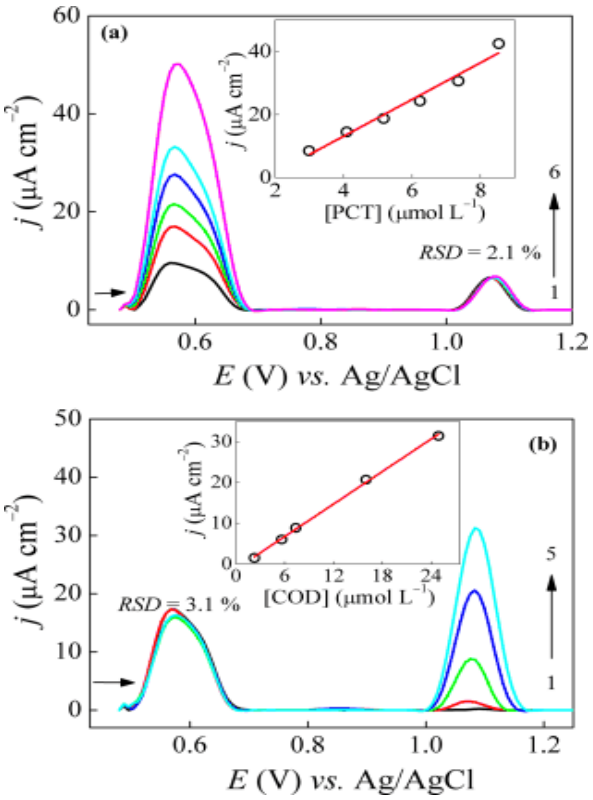

Figure 8. Square-wave voltammograms obtained using the NiONPs-CB-DHP/GCE for various concentrations of: (a) PCT (3.0-8.5 μmol L^{-1}) at a fixed concentration of COD (5.2 μmol L^{-1}); (b) COD (2.3-4.9 μmol L^{-1}) at a fixed concentration of PCT (7.2 μmol L^{-1}). Adapted from [67].

e-ISSN:2319-9849
p-ISSN:2322-0082

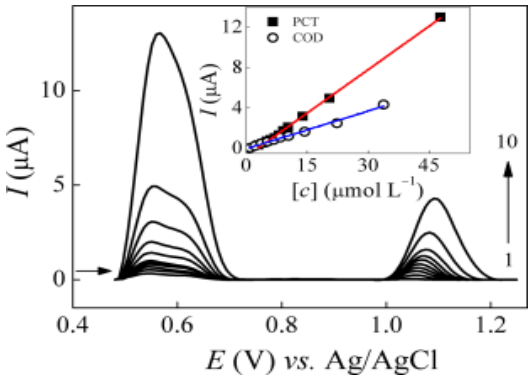

Figure 9. Square wave voltammograms obtained using the NiONPs-CB-DHP/GCE for various concentrations of PCT and COD (1-10): from 3.0 to 47.8 μmol L^{-1} for PCT and from 0.83 to 38.3 μmol L^{-1} for COD. Adapted from [67-70].

The results obtained were therefore compared with previously reported work and the developed biosensor was found to be much better than the first three reported results while having a comparable result with the others. In order to test the effectiveness of the electrode to real sample analysis, two tablets containing known amount (from HPLC analysis) of PCT and COD were employed for the electrochemical analysis and the result obtained by the proposed square wave voltammogram were comparable to the HPLC analysis results. Two equal amounts of urine and human serum samples each spiked with different concentration of PCT and COD, were analyzed using the NiONPs-CB-DHP/GCE electrode and very satisfactory recoveries were obtained for both analytes.

CONCLUSION

The applications of nanomaterials in electrochemical sensors have been highlighted in this article. Nanomaterials such as gold nanoparticles have been shown to act as a label/tag for the amplified detection of DNA, while the large surface area to volume ratio of carbon nanotubes such as multi walled nanotubes have been utilized in improving the response for detection of glucose. ZnONTs, another class of nanotubes, have also been reported as excellent nanomaterial for highly sensitive and selective detection of glucose by immobilizing glucose oxidase. The synergic effect of nickel oxide nanoparticles together with carbon black-dihexadecylphosphate has also enhanced the significantly the signal responses for simultaneous detection of paracetamol and codeine. There are a lot of other nanomaterials' application in electrochemical sensors that were not presented, however, it is hoped that the information provided will stimulate researchers into in-depth study of nanomaterial applications in developing viable electrochemical sensors.

REFERENCES

1. Colvin VL. The potential environmental impact of engineered nanomaterials. Nature Biotechnology 2003;21:1166-1170.
2. Rao CNR, et al. Graphene: the new two-dimensional nanomaterial. Angewandte Chemie International Edition 2009;48:7752-7777.
3. Shi X, et al. Cell entry of one-dimensional nanomaterials occurs by tip recognition and rotation. Nature nanotechnology 2011;6:714-719.
4. Golanski A. Release-ability of nano fillers from different nanomaterials (toward the acceptability of nanoproduct). Journal of Nanoparticle Research 2012;14:1-9.
5. An K and Somorjai GA. Size and shape control of metal nanoparticles for reaction selectivity in catalysis. Chem Cat Chem 2012;4:1512-1524.
6. Li W, et al. CuTe nanocrystals: shape and size control, plasmonic properties, and use as SERS probes and photothermal agents. Journal of the American Chemical Society 2013;135;7098-7101.
7. Niikura K, et al. Gold nanoparticles as a vaccine platform: influence of size and shape on immunological responses in vitro and in vivo. ACS Nano 2013;7:3926-3938.
8. Song S, et al. Functional nanoprobes for ultrasensitive detection of biomolecules. Chemical Society Reviews 2010;39:4234-4243.
9. Mout R, et al. Surface functionalization of nanoparticles for nanomedicine. Chemical Society Reviews 2012;41:2539-2544.
10. Pelaz B, et al. Surface functionalization of nanoparticles with polyethylene glycol: effects on protein adsorption and cellular uptake. ACS Nano 2015;9:6996-7008.
11. Chen D, et al. Graphene oxide: preparation, functionalization, and electrochemical applications. Chemical reviews 2012;112:6027-6053.

e-ISSN:2319-9849
p-ISSN:2322-0082

12. Kavosi B, et al. Au nanoparticles/PAMAM dendrimer functionalized wired ethyleneamine-viologen as highly efficient interface for ultra-sensitive α-fetoprotein electrochemical immunosensor. Biosensors and Bioelectronics 2014;59:389-396.

13. Jia X, et al. Engineering the bio electrochemical interface using functional nanomaterials and microchip technique toward sensitive and portable electrochemical biosensors. Biosensors and Bioelectronics 2016;76:80-90.

14. Pérez-Lorenzo M. Palladium Nanoparticles as Efficient Catalysts for Suzuki Cross-Coupling Reactions. The Journal of Physical Chemistry Letters 2012;3:167-174.

15. Rao JP. Polymer nanoparticles: Preparation techniques and size-control parameters. Progress in Polymer Science 2011;36:887-913.

16. Mudshinge SR, et al. Nanoparticles: Emerging carriers for drug delivery. Saudi Pharmaceutical Journal 2011;19:129-141.

17. Neethirajan S and Jayas D. Nanotechnology for the Food and Bioprocessing Industries. Food Bioprocess Technol 2011;4:39-47.

18. Kong T, et al. An amperometric glucose biosensor based on the immobilization of glucose oxidase on the ZnO nanotubes, Sensors and Actuators B: Chemical 2011;138:344-350.

19. Langhus DL. Analytical Electrochemistry. 2nd edn. Journal of Chemical Education 2011;78:457.

20. Banica FG. Chemical sensors and biosensors: fundamentals and applications. John Wiley & Sons, 2012.

21. Ronkainen NJ, et al. Electrochemical biosensors, Chemical Society Reviews 2010;39:1747-1763.

22. Zhang D and Liu Q. Biosensors and bioelectronics on smartphone for portable biochemical detection. Biosensors and Bioelectronics 2016;75:273-284.

23. Voiculescu I and Nordin AN. Acoustic wave based MEMS devices for biosensing applications. Biosensors and Bioelectronics 2012;33:1-9.

24. Cao J, et al. Gold nanorod-based localized surface plasmon resonance biosensors: A review. Sensors and Actuators B: Chemical 2014;195:332-351.

25. Ferrier DC. Micro- and nano-structure based oligonucleotide sensors. Biosensors and Bioelectronics 2015;68:798-810.

26. Wang Y, et al. Carbon quantum dots: synthesis, properties and applications. Journal of Materials Chemistry C 2014;2:6921-6939.

27. Liang Q, et al. Easy synthesis of highly fluorescent carbon quantum dots from gelatin and their luminescent properties and applications. Carbon 2013;60:421-428.

28. Hansen JA, et al. Quantum-Dot/Aptamer-Based Ultrasensitive Multi-Analyte Electrochemical Biosensor. Journal of the American Chemical Society 2006;128:2228-2229.

29. Ellington AW and Szostak JW. In vitro selection of RNA molecules that bind specific ligands. Nature 1990;346:818-822.

30. Ikebukuro K, et al. Novel electrochemical sensor system for protein using the aptamers in sandwich manner. Biosensors and Bioelectronics 2005;20:2168-2172.

31. Wang J. Nanomaterial-Based Amplified Transduction of Biomolecular Interactions. Small 2005;1:1036-1043.

32. Nutiu R and Li Y. Structure-Switching Signaling Aptamers. Journal of the American Chemical Society 2003;125:4771-4778.

33. Levy M, et al. Quantum-Dot Aptamer Beacons for the Detection of Proteins. Chem Bio Chem 2005;6:2163-2166.

34. Grimsdale AC and Müllen K. The Chemistry of Organic Nanomaterials. Angewandte Chemie International Edition 2005;44:5592-5629.

35. Dai Z, et al. Nanoparticle-Based Sensing of Glycan−Lectin Interactions. Journal of the American Chemical Society 2006;128:10018-10019.

36. Taton TA, et al. Two-Color Labeling of Oligonucleotide Arrays via Size-Selective Scattering of Nanoparticle Probes. Journal of the American Chemical Society 123:5164-5165.

37. Joginadha SM, et al. Further characterization of the saccharide specificity of peanut (Arachis hypogaea) agglutinin. Carbohydrate Research 1991;213:59-67.

38. Zhang X, et al. A New Signal-On Photoelectrochemical Biosensor Based on a Graphene/Quantum-Dot Nanocomposite Amplified by the Dual-Quenched Effect of Bipyridinium Relay and AuNPs. Chemistry - A European Journal 2012;18:16411-16418.

39. Castañeda MT, et al. Electrochemical sensing of DNA using gold nanoparticles. Electroanalysis 2007;19:743-753.

40. Niu X, et al. A novel electrochemical sensor of bisphenol A based on stacked graphene nanofibers/gold nanoparticles composite modified glassy carbon electrode. Electrochimica Acta 2013;98:167-175.

e-ISSN:2319-9849
p-ISSN:2322-0082

41. Kawde AN and Wang J. Amplified Electrical Transduction of DNA Hybridization Based on Polymeric Beads Loaded with Multiple Gold Nanoparticle Tags. Electroanalysis 2004;16:101-107.

42. Wang J, et al. Metal Nanoparticle-Based Electrochemical Stripping Potentiometric Detection of DNA Hybridization. Analytical Chemistry 2001;73:5576-5581.

43. Thanh NTK and Rosenzweig Z. Development of an Aggregation-Based Immunoassay for Anti-Protein a Using Gold Nanoparticles. Analytical Chemistry 2002;74:1624-1628.

44. Kisak ET, et al. Self-Limiting Aggregation by Controlled Ligand−Receptor Stoichiometry. Langmuir 2000;16:2825-2831.

45. Taton TA, et al. Scanometric DNA Array Detection with Nanoparticle Probes. Science 2000;289:1757-1760.

46. Patolsky F, et al. Dendritic amplification of DNA analysis by oligonucleotide-functionalized Au-nanoparticles Chemical Communications 2000; pp: 1025-1026.

47. Ting SL, et al. Graphene quantum dots functionalized gold nanoparticles for sensitive electrochemical detection of heavy metal ions. Electrochimica Acta 2015:172:7-11.

48. Sun G, et al. Ultrasensitive electrochemical immunoassay for carcinoembryonic antigen based on three-dimensional macroporous gold nanoparticles/graphene composite platform and multienzyme functionalized nanoporous silver label. Analytica Chimica Acta. 2013;775:85-92.

49. Mani V, et al. Direct electrochemistry of glucose oxidase at electrochemically reduced graphene oxide-multiwalled carbon nanotubes hybrid material modified electrode for glucose biosensor. Biosensors and Bioelectronics 2013;41:309-315.

50. Han C, et al. A multiwalled-carbon-nanotube-based biosensor for monitoring microcystin-LR in sources of drinking water supplies. Advanced Functional Materials 2013;23:1807-1816.

51. Kong J, et al. Nanotube Molecular Wires as Chemical Sensors. Science 2000:287:622-625.

52. Wang SW, et al. A novel multi-walled carbon nanotube-based biosensor for glucose detection. Biochemical and Biophysical Research Communications 2003;311:572-576.

53. Schuhmann W. Biosensors: Microelectrochemical devices. In: Lambrechts M, Sansen W (eds.), Institute of Physics Publishing, Bristol 1992; p: 304.

54. Hassan Y. King Faisal Specialist Hospital and Research Centre, Riyadh, Saudi Arabia. Marcel Dekker Inc: New York and Basel. Journal of the American Chemical Society 2002;124:511-512.

55. Creager S. Electrochemical Sensors in Bioanalysis By Raluca-Ioana Stefan and Jacobus Frederick Van Staden, University of Pretoria, Pretoria, South Africa. 2001; p: 288.

56. Pérez-Alonso F, et al. Effect of carbon nanotube diameter for the synthesis of Fe/N/multiwall carbon nanotubes and repercussions for the oxygen reduction reaction. Journal of power sources 2013;240:494-502.

57. Mani V, et al. Direct electrochemistry of myoglobin at reduced graphene oxide-multiwalled carbon nanotubes-platinum nanoparticles nanocomposite and biosensing towards hydrogen peroxide and nitrite. Biosensors and Bioelectronics 2014;53:420-427.

58. Gracia-Espino E, et al. Temperature Dependence of Sensors Based on Silver-Decorated Nitrogen-Doped Multiwalled Carbon Nanotubes. Journal of Sensors 2016.

59. Chen GE. Preparation and characterization of a novel hydrophilic PVDF/PVA UF membrane modified by carboxylated multiwalled carbon nanotubes, Polymer Engineering & Science 2016; p: 201.

60. Zhu X, Electrochemical study of the effect of nano-zinc oxide on microperoxidase and its application to more sensitive hydrogen peroxide biosensor preparation. Biosensors and Bioelectronics 2007;22:1600-1604.

61. Zhao ZX, et al. A novel aerometric biosensor based on ZnO: Co nanoclusters for bio sensing glucose. Biosensors and Bioelectronics 2007;23:135-139.

62. Zhao ZX, et al. Aerometric glucose biosensor based on self-assembly hydrophobin with high efficiency of enzyme utilization. Biosensors and Bioelectronics 2007;22:3021-3027.

63. Wang L, et al. ZnO nanorod gas sensor for ethanol detection. Sensors and Actuators B: Chemical 2012;162:237-243.

64. Khoang ND, et al. Design of SnO2/ZnO hierarchical nanostructures for enhanced ethanol gas-sensing performance. Sensors and Actuators B: Chemical 2012;174:594-601.

65. Yayu Z, et al. Pt/ZnO nanoarray nanogenerator as self-powered active gas sensor with linear ethanol sensing at room temperature. Nanotechnology 2014;25:115502.

66. Lin Y, et al. Room-temperature self-powered ethanol sensing of a Pd/ZnO nanoarray nanogenerator driven by human finger movement. Nanoscale 2014;6:4604-4610.

e-ISSN:2319-9849
p-ISSN:2322-0082

67. Wang X, et al. Gas sensors, thermistor and photodetector based on ZnS nanowires. Journal of Materials Chemistry 2012;22:6845-6850.

68. Batista P, et al. An Electrochemical Sensor for the Simultaneous Determination of Paracetamol and Codeine Using a Glassy Carbon Electrode Modified with Nickel Oxide Nanoparticles and Carbon Black. Electroanalysis. 2015;27:2214-2220.

69. Beitollahi H, et al. Nanomolar and Selective Determination of Epinephrine in the Presence of Norepinephrine Using Carbon Paste Electrode Modified with Carbon Nanotubes and Novel 2-(4-Oxo-3-phenyl-3,4-dihydro-quinazolinyl)-N′-phenyl-hydrazinecarbothioamide. Analytical Chemistry 2000;80:9848-9851.

70. Rastgar S, et al. Nickel hydroxide nanoparticles-reduced graphene oxide nanosheets film: Layer-by-layer electrochemical preparation, characterization and rifampicin sensory application. Talanta 2014;119:156-163.